Materials Science Forum Vols. 289-292 (1998) pp. 813-828

Application of Measurement Models for Interpretation of Impedance Spectra for Corrosion

M.E. Orazem[1], P.T. Wojcik[1], M. Durbha[1],
I. Frateur[2] and L.H. Garcia-Rubio[3]

[1] Department of Chemical Engineering, University of Florida, Gainesville, Florida 32611, USA

[2] UPR 15 du CNRS "Physique des Liquides et Electrochimie", Université Pierre et Marie Curie, Tour 22, 4 Place Jussieu, F-75252 Paris Cedex 05, France

[3] Department of Chemical Engineering, University of South Florida, Tampa, Florida 33620, USA

Keywords: Impedance Spectroscopy, Measurement Models, Error Analysis, Polarization Resistance

Abstract

Experimental identification of errors has allowed enhanced interpretation of a wide variety of spectroscopy techniques, including measurements for electrochemical systems for which detailed process models are available. The physicochemical models available for corrosion systems, however, are typically not sufficiently detailed to represent adequately impedance data to within the experimentally determined noise level of the measurement. Even in the absence of detailed physicochemical models, enhanced interpretation of corrosion processes is possible through the use of measurement models which can account quantitatively for differences in surface reactivities. In this paper, the necessary steps for the quantification of corrosion processes using the measurement model approach of Agarwal *et al.* are described. The stationary stochastic error contribution to impedance spectra is identified from replicated measurements. Presence of a bias error contribution, caused, for example, by instrumental artifacts and non-stationary behavior, is identified from application of the Kramers-Kronig transforms. The zero and high frequency limits obtained through the measurement model are used to determine the polarization resistance in a way that accounts for the experimentally determined error structure. The results of this procedure, weighted by an appropriate statistical analysis, can be used to monitor electrochemical systems as functions of time or process conditions. The approach described herein is validated for model systems, such as the reduction of ferricyanide on platinum for which accurate process models are available. The corrosion examples presented here involve the transient growth of corrosion-product films on copper in synthetic seawater and on cast iron in Evian water.

Introduction

Interpretation of impedance data requires, in principle, both a model which describes the physics of the system under study and a quantitative assessment of the error structure of the measurement.[1-3] The experimental difficulty of quantifying the error structure for electrochemical impedance spectroscopy had, until recently, prevented application of an error analysis approach for interpretation of spectra. The error structure for most radiation-based spectroscopic measurements such as absorption spectroscopy and light scattering can be readily identified.[4-6] The error analysis approach has been successful for some optical spectroscopy techniques because these systems lend themselves to replication and, therefore, to the independent identification of the different errors that contribute to the total variance of the measurements. In contrast, the stochastic contribution to the error structure of electrochemical impedance spectroscopy measurements cannot generally be obtained from the standard deviation of repeated measurements because even a mild non-stationary behavior introduces a significant time-varying bias contribution to the error. Recent

advances in the use of measurement models for filtering lack of replicacy have made possible experimental determination of the stochastic and bias contributions to the error structure for impedance measurements.[7-16]

The measurement model approach for identification of error structure, previously used for optical spectroscopies,[4-6] has recently been applied to electrochemical systems.[7-16] Enhanced interpretation of impedance spectra was demonstrated for some systems for which detailed process models were available. For example, using normal weighting strategies impedance spectra for n-GaAs diodes, information concerning deep-level states could not be obtained; whereas, evaluation of the error structure allowed interpretation in terms of concentrations and energy levels of deep-level electronic states.[8,17,18] Similar improvement was demonstrated for interpretation of electrohydrodynamic impedance spectra in terms of transport properties.[16]

Such enhanced interpretation was possible for the GaAs system and the electrohydrodynamic impedance system because sophisticated process models were available which could be used to interpret the measurements in terms of well-defined physical properties. The objective of this work was to explore how the error analysis approach made possible by use of the measurement model can be used for corrosion systems for which detailed process models are often unavailable.

Classification of Measurement Errors

The residual errors ε_{res} that arise when a model is regressed to experimental data have systematic and stochastic contributions, *i.e.*,[1-3]

$$\varepsilon_{res} = Z_{exp} - Z_{mod} = \varepsilon_{systematic} + \varepsilon_{stochastic} \quad (1)$$

The contribution to the total variance of the stochastic errors is in two parts: a stationary component with mean zero and a frequency-dependent variance and a non-stationary component that may result in bias or drift. The stationary stochastic errors were assumed in this work to have a Gaussian distribution around a mean value of zero. Systematic errors can arise from model inadequacies or from experimental bias. The error analysis employed in this work involves quantification of stationary stochastic errors and experimental bias errors. Experimental bias errors were assumed to be those errors which cause the data to be inconsistent with the Kramers-Kronig relations. As defined, the term experimental bias error does not include contributions from model inadequacy, but does include contributions from non-stationary stochastic errors and both stationary and non-stationary systematic experimental errors. Changes in the system characteristics during the course of the measurement can cause non-stationary experimental bias errors, and instrumental artifacts can cause stationary experimental bias errors. As described in the subsequent section, the measurement model was used to filter lack of replicacy between repeated measurements and to identify consistency with the Kramers-Kronig relations.

Applications of Measurement Models to Corrosion

The measurement model facilitates design of experiments and, for systems for which detailed process models are unavailable, can be used to obtain asymptotic values which provide rough estimations of corrosion rates.

Experimental Design

To be useful as a monitor of corrosion processes, the impedance data obtained should allow ready interpretation in terms of physical properties. If the time constant for the transient process is of the same order as the time required for the impedance scan, the non-stationarity of the system will introduce bias errors in the impedance measurement and will cause the data to be inconsistent with

the Kramers-Kronig relations. The use of the measurement model concept to assess the error structure of the impedance scans allows identification of the portion of the measurement that is unaffected by experimental bias errors.[14] The second benefit of the error analysis approach is identification of the stationary stochastic component of the error structure.[13] This information can be used to direct modification of the experimental design to minimize bias and stochastic errors. For example, bias errors caused by nonstationarity can be reduced by decreasing the time required for the measurement. One approach is to decrease the integration time at each frequency, but this reduction of bias errors is at the expense of increasing the noise level of the measurement. Another approach is to reduce the number of frequencies sampled, but this strategy has the effect of reducing the degree of freedom for the regression. A third approach is to eliminate a source of noise in the system, for example, by using a low-pass filter to reduce the high-frequency noise in the signals input to the frequency response analyzer. Selection of an appropriate strategy to reduce experimental time requires quantitative assessment of the effect of each strategy on the error characteristics, and this assessment is provided by the measurement model approach.[7,13,14] The above discussion was oriented towards use of digital frequency response analyzers such as the Solartron series, but similar arguments can be developed for other impedance measurement techniques such as phase-sensitive detection (using lock-in amplifiers) and applications of fast Fourier transforms.

Estimation of Asymptotic Values

In addition to its use to quantify the noise level of the measurement and to assess consistency with the Kramers-Kronig relations, the measurement model approach can be used as follows to quantify differences in surface reactivity.

1. The frequency-dependent stationary stochastic component of the error structure was identified following the method presented by Agarwal *et al.*[13] This information was used to weight subsequent regressions.
2. The portion of the spectrum that is consistent with the Kramers-Kronig relations was identified following the method presented by Agarwal *et al.*[14] The error structure found in part 1 above was used to weight the regression. High-frequency data were found in some cases to be corrupted by instrumental artifacts. The low-frequency data were typically found to be consistent with the Kramers-Kronig relations except for data collected under conditions where the system was changing rapidly.
3. The measurement model was regressed to the part of the spectrum found to be consistent with the Kramers-Kronig relations. The regressed parameter values were used to extrapolate the measurement model to the zero frequency limit, and Monte Carlo simulations were performed using the standard deviations of the regressed parameters to estimate the confidence interval for the extrapolation.[14] The polarization impedance was obtained by subtracting the regressed solution resistance from the extrapolated zero frequency value.

Results and Discussion

The emphasis of the present work is on the use of the measurement model for determining zero and high-frequency asymptotes for the impedance response. In this section, an experimental system is described that was used to validate the procedure and examples of its implementation are given.

Verification of Procedure

Data obtained for the reduction of ferricyanide on a Pt rotating disk electrode were used to verify that the procedure described above provides adequate estimation of the polarization impedance.[19,20] The data set used for this purpose was collected at a rotation speed of 120 rpm,

at one quarter of the mass-transfer-limited current, and at a temperature of 25°C. As this system was controlled by mass transfer, it provided a good test of the algorithm. While, in theory, an infinite number of Voigt elements are needed to approximate a Warburg impedance, only a finite number can be obtained from the regression of a Voigt model to the data because stochastic errors (or noise) in the measurement limit the information content of the data.

A process model for the impedance response associated with convective diffusion to a rotating disk, developed by Tribollet and Newman,[21] was modified by Orazem *et al.*[22]

$$Z(\omega) = R_e + \frac{R_t + z_d(\omega)}{1 + (j\omega C)^{\alpha}(R_t + z_d(\omega))} \qquad (2)$$

where

$$[illegible] \qquad (3)$$

The model includes 6 parameters (R_e, R_t, C, α, $z_d(0)$, and Sc) which were obtained by regression to the data. The methods of Agarwal *et al.*[7,13,14] were used to identify the frequency-dependent standard deviation of repeated measurements and to remove data influenced by bias errors that caused inconsistencies with the Kramers-Kronig relations. A weighted non-linear least squares regression was used to fit the process model to the data, and the weighting was provided by the inverse of the experimentally determined variance of the data.

The results of the regression are provided in Fig. 1. The data and the model reveal a high frequency loop associated with the electrode reaction and a low frequency loop corresponding to Warburg behavior. The residual errors for the regression show that the fitting errors are of the order of the noise level of the measurement. The larger deviation and trending evident at frequencies above 100 Hz are attributed to the approximate constant-phase-element model used to account for the electrochemical reaction. The dashed lines in Figs. 1b and 1c represent 95.4 percent confidence intervals (2 times the experimentally determined standard deviation of the measurement) scaled to the real and imaginary parts of the impedance, respectively. The standard deviations of the real and imaginary parts were found to be equal, as reported for other spectroscopy systems,[23] and the different appearance of the confidence interval lines in Figs. 1b and 1c are caused by the different scaling used. The 95.4 percent confidence intervals for the data are of the order of 0.3 percent of the real part of the impedance and 1 percent of the imaginary part. As seen in Table 1, the Schmidt number obtained was 1163±39 which is close to the value of 1100±4 obtained by Robertson *et al.* using DC methods and 1155±43 using electrohydrodynamic impedance methods.[24] The residual sum of squares for this fit was 1.561 times the sum of variances. In the context of an F-Test for comparison of variance,[1] the ratio is less than $F_{0.01}$=1.754 which suggests that the hypothesis that the residual sum of squares is statistically different from the sum of variances for the measurement can be rejected. The trending of the residual errors at frequencies above 100 Hz suggests, however, that the model does not adequately describe the high frequency behavior.

Monte Carlo simulations were performed to extrapolate the process model to the zero frequency asymptote. The resulting value of 188.6±0.9 Ω is shown as a diamond in Fig. 1a. The corresponding value obtained by regression of the measurement model, shown in Fig. 2, was 188.3±0.6 Ω. The number of Voigt elements used was the largest that yielded parameter estimates that did not include zero within their 95.4% confidence interval. The regression of the measurement model yielded a normalized residual sum of squares of 1.8691, which was larger than that obtained by the process model. The residual errors shown in Figs. 2b and 2c fell roughly within the confidence interval of the data. In spite of the fact Voigt elements provide only an approximate representation of Warburg

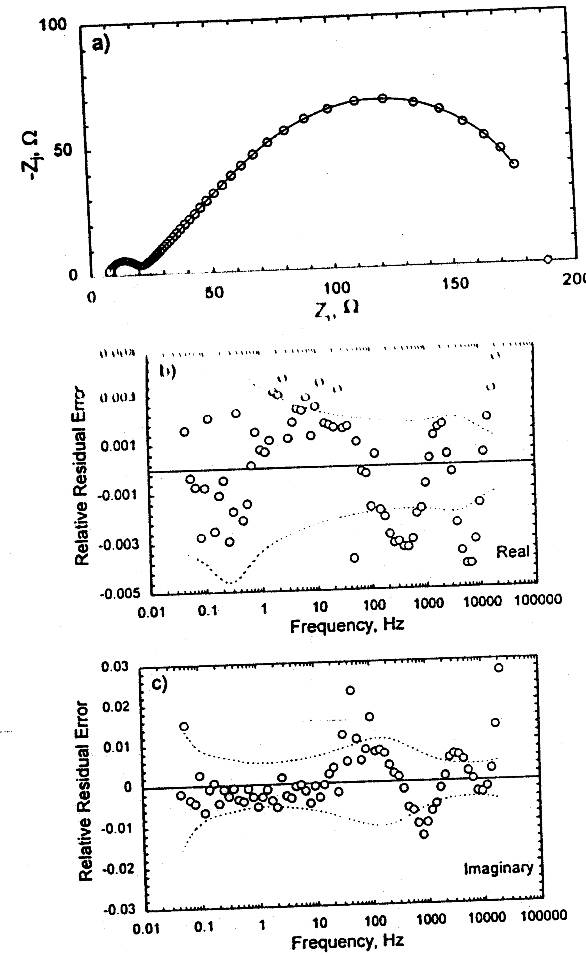

Figure 1. Results of the regression of the process model (equations (2) and (3)) to the data obtained for the reduction of ferricyanide on a Pt disk rotating at 120 rpm and held at ¼ of the mass-transfer-limited current. The regression was weighted by the experimentally determined variance, and data shown by the measurement model to be inconsistent were removed from the regressed data set. The frequency range was 0.0461 Hz to 21.4 kHz. a) impedance plane representation where O represents data used in the regression, ◊ represents the predicted zero-frequency asymptote, and the line is the regressed fit. b) and c) relative residual error for the regression where the dashed lines represent the bounds for the 95.4% confidence interval for the measurement (*i.e.*, $\pm 2\sigma / \hat{Z}_r$ and $\pm 2\sigma / \hat{Z}_j$, respectively).

Table 1. Comparison of regression results obtained using the measurement and process models. The shaded area represents conditions under which both models could be regressed to the data.

Measurement Model				Process Model				Error %
#data	Lowest Frequency, Hz	#Voigt elements	NSSQ*	R_{sol}, Ω	Z(0) , Ω	NSSQ*	R_{sol}, Ω	Sc	Z(0) , Ω	
69	0.0461	9	1.8691	6.96 ± 0.03	188.3 ± 0.6	1.561	7.2548 ± 0.0071	1163 ± 39	188.6 ± 0.9	-0.19
63	0.146	9	1.8109	6.95 ± 0.04	187.4 ± 0.6	1.434	7.2548 ± 0.0075	1166 ± 79	188.7 ± 1.9	-0.66
58	0.381	11	0.8424	6.70 ± 0.12	184.2 ± 1.7	2.739	7.2548 ± 0.0078	1127 ± 208	187.8 ± 5.4	-1.94
57	0.461	11	0.8744	6.72 ± 0.11	185.6 ± 2.2	2.99	7.2548 ± 0.0079	1154 ± 288	188.5 ± 6.9	-1.55
56	0.559	11	0.9977	6.73 ± 0.11	182.5 ± 3.1	...Regression Failed...				
53	0.993	9	1.895	6.81 ± 0.07	151.0 ± 2.5					
48	2.59	9	1.3026	6.80 ± 0.07	139 ± 38					
43	6.77	8	1.6767	6.84 ± 0.06	104 ± 23					
38	17.7	7	1.7196	6.78 ± 0.08	54.5 ± 1.6					
33	46.1	7	0.9235	6.70 ± 0.10	40.9 ± 1.2					
28	120.	6	0.4807	6.46 ± 0.19	30.7 ± 0.6					
23	314.08	5	0.7675	6.70 ± 0.10	25.9 ± 0.3					

* Residual sum of squares normalized by the independently determined sum of variances for the measurement.

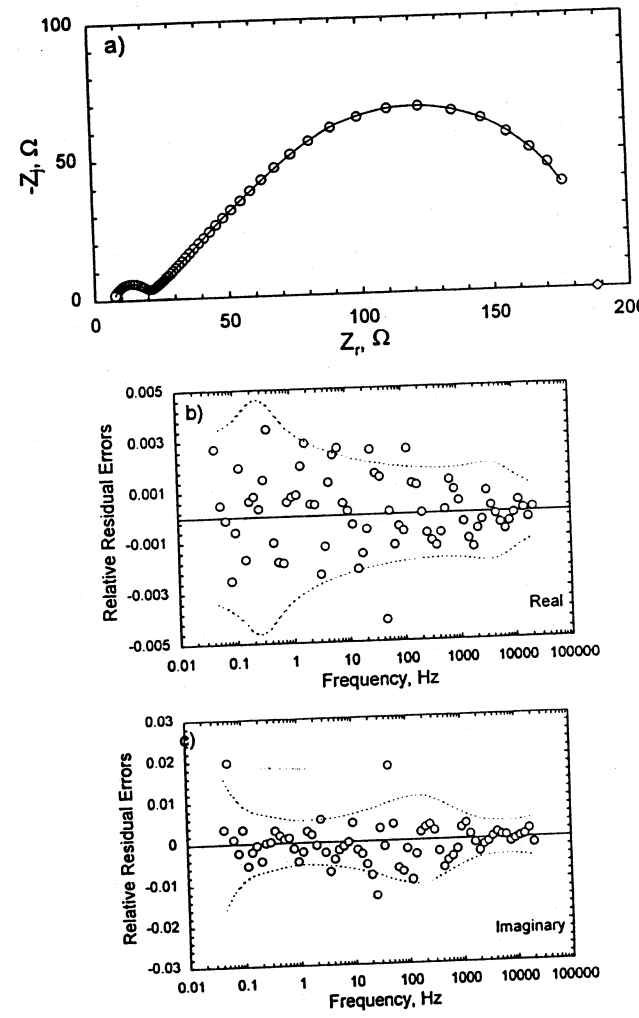

Figure 2. Results of the regression of the measurement model to the data presented in Figure 1. The frequency range was 0.0461 Hz to 21.4 kHz. a) impedance plane representation where O represents data used in the regression, ◊ represents the predicted zero-frequency asymptote, and the line is the regressed fit. b) and c) relative residual error for the regression where the dashed lines represent the bounds for the 95.4% confidence interval for the measurement (*i.e.*, $\pm 2\sigma / \hat{Z}$, and $\pm 2\sigma / \hat{Z}_j$, respectively).

behavior, the zero frequency asymptotes and solution resistances obtained by the two models were in good agreement. The solution resistance obtained by using the process (Warburg) model was 7.2548±0.0071 Ω; whereas that obtained using the measurement model was 6.96±0.03 Ω.

The fit and extrapolation of the process model to a reduced data set is shown in Fig. 3. The lowest frequency included in the regression was 0.461 Hz. The corresponding results from regression of the measurement model with eleven Voigt elements are shown in Fig. 4. The regression results are shown in Table 1. Both process and measurement models could be used successfully to extrapolate the data, and the results obtained agreed to within 1.55 percent.

The process model could not be used to obtain a full set of parameters with a data set reduced further than that shown in Figs. 3 and 4 because the resulting confidence interval for the Schmidt number included zero. As the measurement model based on a superposition of Voigt elements is more general, it could be used to provide extrapolations of more severely reduced data sets, as shown in Figs. 5a and 5b. A summary of the comparison between asymptotic values predicted by the process and measurement models is shown in Fig. 6. As the process model describes more completely the low-frequency behavior of the system, the results obtained from the process model are considered to be more reliable. Within the frequency range that was sufficiently complete as to allow use of the process model for extrapolations, the measurement model gave asymptotic values that were in good agreement with those obtained from the process model. The asymptotic values obtained by fitting the measurement model to a more severely truncated data set, however, were lower than the expected value. This result can be expected because deletion of low-frequency data results in a loss of information from low-frequency processes. It should be noted that the confidence interval for the extrapolated values, obtained using the standard deviations of regressed parameters, did not provide an accurate indication of the uncertainty associated with missing data.

This work shows that, in spite of the fact Voigt elements provide only an approximate representation of Warburg behavior, when sufficient low-frequency data were included that the Warburg model could be regressed to the data, the zero and high frequency asymptotes obtained by the two models were in good agreement. The measurement model therefore provides a useful tool for approximate analysis of impedance data under conditions that an appropriate process model is unavailable. The measurement model does not, however, provide an alternative to collecting data over a frequency range sufficient to sample all relevant electrochemical phenomena.

Corrosion of Copper in Synthetic Seawater

The objective of the experiment was to explore the reactivity of the copper coupon as a function of time and as a function of jet velocity.[25-27] A PAR 273 potentiostat was used to monitor the corrosion potential and, at regular intervals, to conduct impedance scans. The impedance measurements were conducted using a Solartron 1260 frequency response analyzer, and the impedance scans were obtained at the zero-current condition using the variable-amplitude galvanostatically-modulated impedance technique.[27]

The corrosion potential is presented in Fig. 7a for a copper disk subjected to a submerged impinging jet of aerated synthetic sea-water at 1 m/s. The transient presented in Fig. 7a represents the first 24 hours of a 480 hour duration experiment. The variable-amplitude galvanostatic method was used to monitor the corrosion system at the open-circuit condition at regular intervals. Impedance data are presented in Fig. 7b. As shown in Fig. 7a, the trends in corrosion potential were unaffected by the impedance scans. The impedance scans given in Fig. 7b show that the surface reactivity changed dramatically over the course of 24 hours.

The polarization impedance and its confidence interval were obtained by Monte Carlo simulations using the parameters and associated confidence intervals obtained by regression of the measurement model. The goal of this effort was to assess the reactivity of the corrosion system in the absence of a

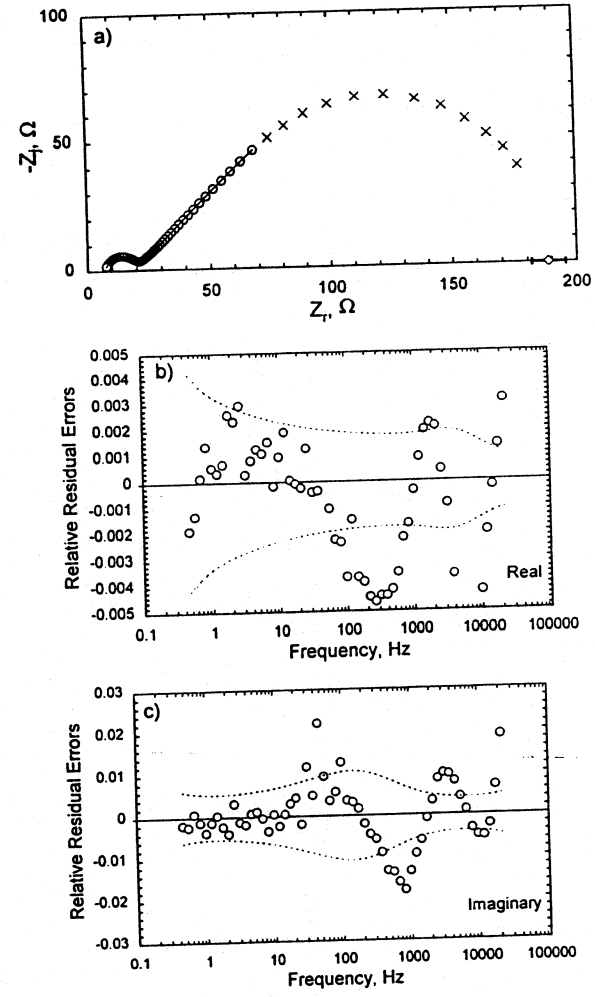

Figure 3. Results of the regression of the process model (equations (2) and (3)) to the data presented in Figure 1. The frequency range was 0.461 Hz to 21.4 kHz. a) impedance plane representation where O represents data used in the regression, × represents data removed from the regression, ◊ represents the predicted zero-frequency asymptote, and the line is the regressed fit. b) and c) relative residual error for the regression where the dashed lines represent the bounds for the 95.4% confidence interval for the measurement (*i.e.*, $\pm 2\sigma / \hat{Z}_r$ and $\pm 2\sigma / \hat{Z}_j$, respectively).

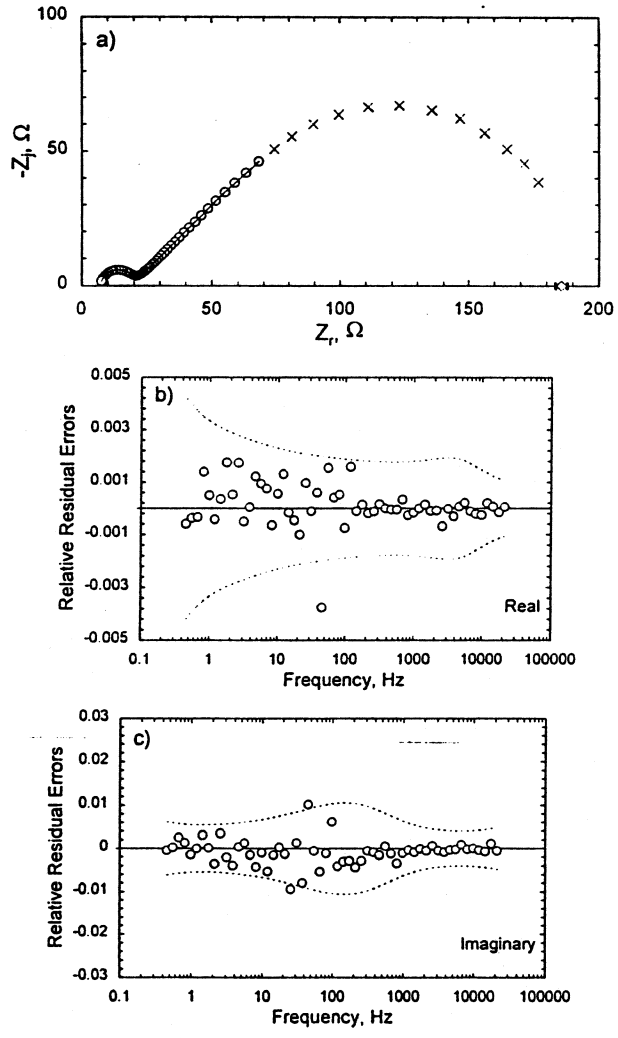

Figure 4. Results of the regression of the measurement model to the data presented in Figure 3. The frequency range was 0.461 Hz to 21.4 kHz. a) impedance plane representation where O represents data used in the regression, × represents data removed from the regression, ◊ represents the predicted zero-frequency asymptote, and the line is the regressed fit. b) and c) relative residual error for the regression where the dashed lines represent the bounds for the 95.4% confidence interval for the measurement (*i.e.*, $\pm 2\sigma/\hat{Z}_r$ and $\pm 2\sigma/\hat{Z}_i$, respectively).

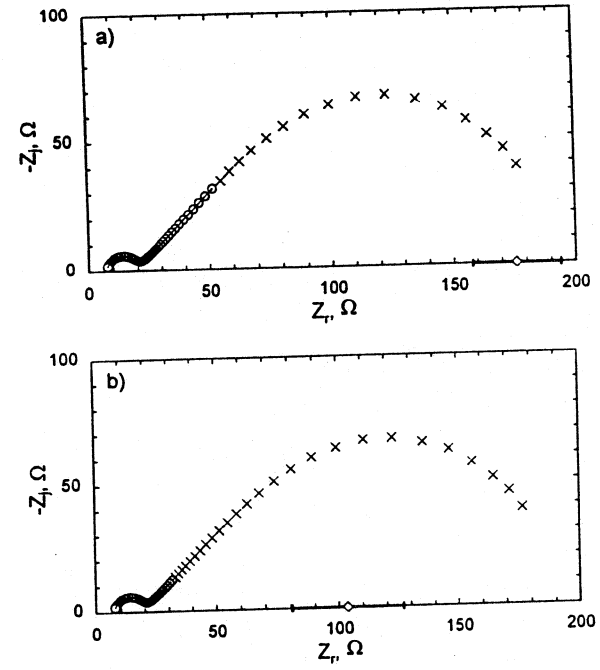

Figure 5. Results of the regression of the measurement model to the data presented in Figure 1 where O represents data used in the regression, × represents data removed from the regression, ◊ represents the predicted zero-frequency asymptote, and the line is the regressed fit. a) The regressed frequency range was 0.993 Hz to 21.4 kHz. b) The regressed frequency range was 6.77 Hz to 21.4 kHz.

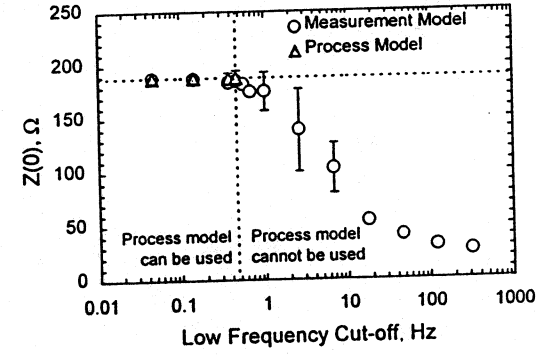

Figure 6. Comparison of the asymptotic values obtained by the measurement model to those obtained using the established process model for this system as a function of the lowest frequency used in the regression.

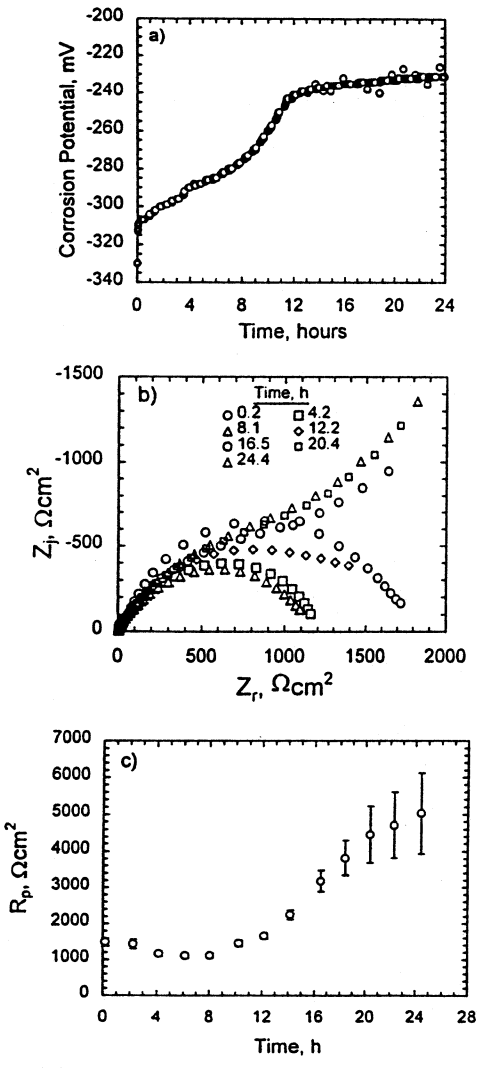

Figure 7. Results obtained for a copper disk subjected to an impinging jet of synthetic sea water with a jet velocity of 1 m/s for 24 hours. a) corrosion potential as a function of time, b) impedance plane representations of impedance spectra obtained using the variable-amplitude galvanostatic modulation, and c) polarization impedance obtained using the techniques presented in this paper.

detailed process model. Results are presented in Fig. 7c for the polarization impedance as a function of time for the impedance data shown in Fig. 7b. The polarization impedance increased from an initial value of roughly 1,500 to 10,000 Ωcm^2. The impedance decreased initially due to removal of the native oxide layer and then increased as the films associated with the corrosion products formed and grew. The role of the measurement model for evaluating consistency with the Kramers-Kronig relations is evident in that the apparent zero frequency asymptote of the scan obtained at 0.2 hours (Fig. 6b) was 1,800 Ωcm^2; whereas, the corresponding polarization impedance shown in Fig. 7c obtained by the analysis outlined above was 1,500 Ωcm^2. The low frequency data were corrupted by nonstationary behavior, but a polarization impedance could still be obtained from the portion of the data that satisfied the Kramers-Kronig relations. The use of polarization impedance to monitor the influence of changes in pH and jet velocity for this system is illustrated by Fig. 8.

Cast Iron in Evian Water

The objective of this work was to study the effect of chlorination on the corrosion of cast iron pipes containing municipal drinking water.[28] The electrochemical instrumentation consisted of a Solartron 1287 potentiostat-galvanostat and a Solartron 1250 Frequency Response Analyzer. The frequency range used was 64 kHz to a few mHz. The experiments were performed with a rotating disk electrode machined from a cast iron potable water pipe. The electrolyte was the commercial Evian water, used as delivered. The temperature was fixed at 20°C. Other experimental details are presented in reference 28. Results obtained in the absence of chlorination are presented in Fig. 9. The polarization resistance obtained using the measurement model technique is in good agreement with that obtained using a 9-parameter process model which included the influence of a porous film on anodic and cathodic reactions. The Ohmic resistance obtained from the measurement model was in good agreement with that obtained from independent measurements.

Conclusions

Even in the absence of detailed physicochemical models, the enhanced error analysis made possible by use of measurement models can play a significant role in the interpretation of impedance spectra. The identification of stochastic and bias errors allows a rational approach toward experimental design which takes into account the various contributions to the error structure. The zero and high-frequency limits obtained through the measurement model were used to determine the polarization resistance in a way that accounted for the experimentally determined error structure. The results of this procedure, weighted by an appropriate statistical analysis, can be used to monitor electrochemical systems as functions of time or process conditions. The approach was validated for the reduction of ferricyanide on platinum, for which accurate process models are available, and demonstrated for the corrosion of copper in synthetic seawater and of cast iron in Evian water.

Acknowledgements

The work was supported by the Office of Naval Research under Grant Numbers N00014-93-I-0056 and N00014-93-I-1113 (A.J. Sedriks, Program Monitor). This work was also supported in part by the National Science Foundation under a US-France Cooperative Research Grant INT-9416713.

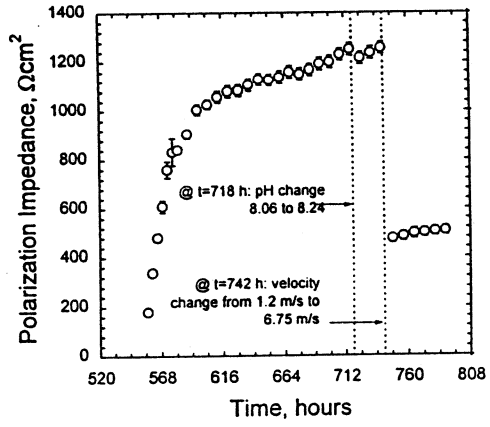

Figure 8. Polarization resistance obtained for a copper disk subjected to an impinging jet of synthetic sea water. The polarization resistance shows a small effect of changing pH at 718 hours and of changing jet velocity at 742 hours.

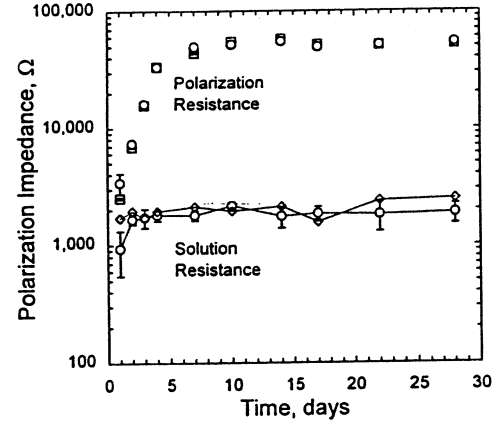

Figure 9. Polarization and solution resistance obtained for a cast iron rotating disk. O) values obtained from measurement model, □) values obtained from a preliminary process model, ◊) independently measured solution resistance.

References

[1] G. E. P. Box and N. R. Draper, *Empirical Model-Building and Response Surfaces,* John Wiley & Sons, Inc., New York, 1987.

[2] Harold W. Sorenson, *Parameter Estimation: Principles and Problems,* Marcel Dekker, Inc., New York, 1980.

[3] G. A. F. Seber, *Linear Regression Analysis,* John Wiley & Sons, New York, 1977, pp. 330-334.

[4] R. W. Christy, *American Journal of Physics,* 40, 1403 (1972).

[5] A. Jutan and L. H. García-Rubio, *Process Control and Quality,* 4, 235 (1993).

[6] L. K. DeNoyer and J. G. Good, *American Laboratory,* March, 1990. Software available from Spectrum Square Associates, Ithaca, NY, 114850.

[7] P. Agarwal, M. E. Orazem, and L. H. García-Rubio, *J. Electrochem. Soc.,* 139, 1917 (1992).

[8] M. E. Orazem, P. Agarwal, A. N. Jansen, P. T. Wojcik, and L. H. García-Rubio, *Electrochimica Acta,* 38, 1903 (1993).

[9] P. Agarwal, O. C. Moghissi, M. E. Orazem, and L. H. García-Rubio, *Corrosion,* 49, 278 (1993).

[10] M. E. Orazem, P. Agarwal, L. H. García-Rubio, *J. Electroanal. Chem.,* 378, 51 (1994).

[11] B. A. Boukamp and J. R. Macdonald, *Solid State Ionics,* 74, 85 (1994).

[12] B. A. Boukamp, *J. Electrochem. Soc.,* 142, 1885 (1995).

[13] P. Agarwal, O. D. Crisalle, M. E. Orazem, and L. H. García-Rubio, *J. Electrochem. Soc.,* 142, 4149 (1995).

[14] P. Agarwal, M. E. Orazem, and L. H. García-Rubio, *J. Electrochem. Soc.,* 142, 4159 (1995).

[15] P. Agarwal, M. E. Orazem, and L. H. García-Rubio, *Electrochimica Acta,* 41, 1017, (1996).

[16] M. E. Orazem, P. Agarwal, C. Deslouis, and B. Tribollet, *J. Electrochem. Soc.,* 143, 948 (1996).

[17] A. N. Jansen, P. T. Wojcik, P. Agarwal, and M. E. Orazem, *J. Electrochem. Soc.,* 143 (1996), 4066-4074.

[18] A. N. Jansen and M. E. Orazem, *J. Electrochem. Soc.,* 143 (1996), 4074-4080.

[19] M. Durbha, *Influence of Non-Uniform Current and Potential Distributions on the Interpretation of Impedance Spectra,* Ph.D. dissertation, University of Florida, Gainesville, 1998.

[20] M. Durbha, M. E. Orazem, C. Deslouis, H. Takenouti, and B. Tribollet, "Current Distribution on a Rotating Disk Electrode Below the Mass-Transfer Limited Current: Influence on the Reduction of Ferricyanide on Pt," in preparation.

[21] B. Tribollet and J. Newman, *J. Electrochem. Soc.,* **130**, 2016 (1983).

[22] M. E. Orazem, C. Deslouis, and B. Tribollet, "Comparison of Impedance Models for Mass Transfer to a Disk Electrode," presented at the 191st Meeting of the Electrochemical Society, Montreal, Canada, May 4-9, 1997, paper in preparation.

[23] M. Durbha, M. E. Orazem, and L. H. García-Rubio, *J. Electrochem. Soc.,* **144** (1997), 48-55.

[24] B. Robertson, B. Tribollet, and C. Deslouis, *J. Electrochem. Soc.,* **135** (1988), 2279.

[25] P. T. Wojcik and M. E. Orazem, Paper #97-435, National Association of Corrosion Engineers, Houston, Texas, 1997.

[26] P. T. Wojcik, E. Charrière, and M. E. Orazem, "Experimental Study of the Erosion-Corrosion of Copper and Copper-Nickel Alloys at the Corrosion Potential and at Anodic Potentials," to be presented at the *Tri-Service Conference on Corrosion,* November 17-21, 1997.

[27] P. T. Wojcik and M. E. Orazem, "Variable-Amplitude Galvanostatically-Modulated Impedance Spectroscopy as a Tool for Assessing Reactivity at the Corrosion Potential without Distorting the Temporal Evolution of the System," *Corrosion*, in press.

[28] C Deslouis, I. Frateur, L. Kiene, Y. Levi, and B. Tribollet, "Corrosion Study of Cast Iron Pipes in Water Distribution Systems by Impedances: Application to Chlorine Consumption," presented at *Electrochemical Methods for Corrosion Research, EMCR 97,* Trento, Italy, August 25-29, 1997.